NASA Technical Memorandum 81610

Core Noise Measurements from a Small, General Aviation Turbofan Engine

Meyer Reshotko and Allen Karchmer
Lewis Research Center
Cleveland, Ohio

Prepared for the
One-hundredth Meeting of the Acoustical Society of America
Los Angeles, California, November 17-21, 1980

NASA

CORE NOISE MEASUREMENTS FROM A SMALL, GENERAL AVIATION TURBOFAN ENGINE

by

Meyer Reshotko* and Allen Karchmer*

National Aeronautics and Space Administration
Lewis Research Center
Cleveland, Ohio 44135

SUMMARY

As part of a program to investigate combustor and other core noises, simultaneous measurements of internal fluctuating pressure and far field noise were made with a JT15D turbofan engine. Acoustic waveguide probes, located in the engine at the combustor, at the turbine exit and in the core nozzle wall, were used to measure internal fluctuating pressures. Low frequency acoustic power determined at the core nozzle exit corresponds in level to the far-field acoustic power at engine speeds below 65% of maximum, the approach condition. At engine speeds above 65% of maximum, the jet noise dominates in the far-field, greatly exceeding that of the core. From coherence measurements, it is shown that the combustor is the dominant source of the low frequency core noise. The results obtained from the JT15D engine were compared with those obtained previously from a YF102 engine, both engines having reverse flow annular combustors and being in the same size class.

*Aerospace Engineer, Fluid Mechanics and Acoustics Division

INTRODUCTION

In the past several years considerable progress has been made in reducing the noise generated by subsonic CTOL aircraft gas turbine engines. The two largest sources of engine noise, the fan and the jet exhaust, can be reduced sufficiently to comply with federal noise regulations. Further reductions of these sources may not reduce the overall engine noise because a new acoustic threshold has been reached. This threshold level is composed of noise generated from heretofore inadequately understood sources within the engine core. One of the most likely sources of far field noise originating from the engine core is the combustion process where large amounts of chemical energy are released.

At the NASA Lewis Research Center, an extensive program is being conducted to determine the sources and characteristics of combustion noise and its propagation through the engine core to the far field. In part, the experimental phase of this program has been conducted with a Lycoming YF102 turbofan engine (Ref. 1). Results obtained from direct internal and external spectral measurements indicate that below a limiting condition (60% of maximum fan speed for this engine), low frequency core noise contributes significantly to the far field noise (Ref. 1). Furthermore, it has been shown by use of correlation and coherence techniques that the combustor is the source of this low frequency core noise (Refs. 2 and 3). In another investigation, acoustic measurements with an auxiliary power unit (APU) produced similar results, showing the combustor to be a contributor to the far field noise at frequencies below 400 Hz (Ref. 4).

The NASA is conducting an inter-center program to better understand the effects of forward velocity on fan noise (Ref. 5 & 6). As part of this program, the Lewis Research Center is conducting static tests on a Pratt & Whitney JT15D turbofan engine. This is a production engine frequently used in general aviation aircraft such as the Cessna Citation. In addition to the fan noise studies, experiments have been conducted with this engine to determine the

characteristics of combustion and other core noises and their propagation through the engine core to the far field. The overall objective of these experiments was to measure the noise in the combustor at various engine operating speeds and determine its propagation downstream (1) through the turbine (2) through the core nozzle, and (3) to the far field.

It is the purpose of this paper to describe the engine acoustic measurement program and to present some of the results obtained. The results consist of single point spectral data measured within the engine core, and two point coherence measurements between various internal engine locations and the acoustic far field. The results obtained from the JT15D measurements are to be compared with those obtained previously from a YF102 engine, both engines having reverse flow annular combustors and being in the same size class.

ENGINE, INSTRUMENTATION, AND DATA PROCESSING

Engine

The Pratt & Whitney JT15D is a bypass ratio 3.3, two spool, turbofan engine with a rated thrust of 9800 newtons. The engine core consists of a compressor in the form of a 16-bladed impeller, a reverse flow annular combustor, and a three stage turbine. The single stage compressor is driven by the high pressure turbine stage, while the fan is directly driven by two low pressure turbine stages. The fan has twenty-eight blades and is 0.534m in diameter.

All tests were conducted using an outdoor engine test stand with the engine centerline 2.9m above a hard surface ground plane. The engine was configured with an inlet control device attached to a flight inlet and separate core and fan exhaust nozzles. The core and fan nozzle areas were .0558 and .0876m^2, respectively. The inlet control device was used to reduce fan tones by providing a cleaner and more uniform inflow than is normally obtained under static test conditions (Ref. 5). A photograph of the engine mounted on the test stand is shown in figure 1.

Measurements were made at ten fan speeds between 33% and 97% of maximum speed (15,840 rpm). A summary of the test conditions, including mass flow, pressures and temperatures in the core engine, is presented in table 1.

Internal Acoustic Probes

Dynamic pressure probes were placed in the engine core at seven different locations (Fig. 2) as follows: one in the combustor; three at the turbine exit, at various circumferential locations; one in the core nozzle entrance; and two, 90^o apart, in the core nozzle exit plane.

The transducers used were conventional 0.635 cm diameter pressure response condenser microphones. To avoid direct exposure of the microphones to the severe

environment within the core, they were mounted outside the engine and the fluctuating pressure in the engine core was communicated to the transducers by "semi-infinite" acoustic waveguides. These waveguide probes are described in detail in reference 1. A photograph of the engine with the probes in place is shown in figure 3.

External Microphones

The far field microphones consisted of an array of sixteen 1.27 cm diameter condenser microphones on a 30.5 m radius circle centered on the exhaust plane of the core nozzle. The microphones were spaced 10^{o} apart from 10^{o} to 160^{o} from the engine inlet axis, and were mounted at ground level to minimize the problems associated with ground reflections.

A near field microphone was placed on a stand at the engine centerline height (2.9 m), 1.65m downstream of the nozzle exit plane and offset 0.95m from the engine centerline.

Data Acquisition and Processing

The signals from the internal probes and far field microphones were FM-recorded on magnetic tape in three-minute record lengths for later processing. The internal probes and far field microphones were calibrated with a pistonphone prior to and at the end of each day's running. The data were analyzed on narrow band and one-third octave band spectrum analyzers which determined pressure level spectra referenced to $2X10^{-5}$Pa.

The coherence and correlation results given in this paper were obtained by off-line processing of the tape-recorded data on a two-channel fast Fourier transform digital signal processor with built-in analog to digital converters and 120 dB/octave anti-aliasing filters. The processor was capable of direct computation of up to 4096 ensemble averages of a 1024 point forward or inverse

Fourier transform to yield either frequency domain (coherence, amplitude and phase spectra, and transfer function) or time domain (correlation) information.

RESULTS & DISCUSSION

The acoustic data were obtained by simultaneous measurements from probes located inside the engine core and microphones placed in the far field. The results are separated into three main categories: 1) single point spectral data measured within the engine core, 2) two point coherence and correlation measurements between various internal engine locations and also between the engine and far field and, 3) a comparison between the JT15D and an earlier tested YT102 engine. Although the engine was operated at ten rotational speeds, data are presented only for several speeds that are considered representative of various conditions in the engine operating cycle.

Single Point Spectral Data

Internal dynamic pressure measurements were made in the combustor, turbine exit and core nozzle exit, and sound pressure levels were measured in the far field of the JT15D engine. Typical one-third octave band dynamic pressure level spectra at these locations are presented in figure 4 for two engine fan speeds, 40% and 87% of maximum. These spectra indicate the magnitude of each signal progressively from one location to another and exhibit the broadband nature of the signal at the lower frequencies, and the tonal content due to the rotating machinery at the higher frequencies. However, these data by themselves do not indicate the origin or the propagation characteristics of the broadband signals and the tones, nor do they indicate whether the probes are measuring acoustic pressure, hydrostatic pressure fluctuations, or some combination of the two. To explore these points, the data for each component will be examined separately in this section, and then by component pairs in the following section.

Combustor - The pressure level spectra presented in figure 5 were obtained by a probe flush mounted in the combustor liner (Fig. 2). In figure 5(a), one-third octave band combustor pressure spectra are presented for five engines speeds at frequencies up to 2000 Hz. The shapes of the spectra are similar for all speeds and as would be expected, the pressure level increases with increasing engine speed. Narrow band spectra for the same speeds and frequency range are shown in figure 5(b). The spectra at all speeds are generally broad-band in nature, however, at 40% of maximum speed and higher there are strong tones of varying magnitude. The frequencies of these tones correspond to the rotational speeds and multiples thereof of the turbomachinery (fan, turbine, etc). A narrow band spectrum taken at 40% of maximum speed and at a frequency range of 0 to 10,000 Hz is shown in figure 6. At 4916 and 9832 Hz respectively, there appear to be two tones of very large magnitude. These tones correspond to the blade passage frequency and second harmonic of the 16 bladed impeller of the centrifugal compressor which are passing through the combustor. This phenomenon is discussed in more detail in reference 7.

In reference 8 it is suggested that combustion noise is directly related to and a prime function of the combustion heat release rate, Q, associated with the combustion process. A plot of the acoustic power as a function of the heat release rate for the JT15D is presented in figure 7. The combustor heat release rate, Q, in this report is determined from the relationship

$$Q = wC_p(\Delta T) \tag{1}$$

where

w combustion air flow rate

C_p specific heat of air

ΔT temperature rise due to combustion

The overall acoustic power levels used herein were inferred from measured

fluctuating pressures obtained within the combustor using the method and assumptions of reference 8. The ten engine operating conditions produce a range in heat release rate that span a factor of six between minimum and maximum. By empirical observation, the data fall into two categories, the first, at the low heat release rates, shows the acoustic power to behave as approximately Q^2, and the second, at the higher heat release rate shows the acoustic power to behave approximately as Q to the first power. The data shown in figure 7 follow the same trends as the data obtained from many different combustors and reported in reference 8.

Core nozzle exit - Pressure level spectra obtained by probes flush mounted in the core nozzle exit are presented in figure 8. In figure 8(a), one-third octave band core nozzle exit pressure spectra are presented for representative speeds at frequencies up to 2000 Hz. Narrow band spectra for the same speeds and frequency range are shown in figure 8(b). The spectra at all speeds are generally broadband in nature, however, at selected speeds there are strong tones of varying magnitude. The frequencies of these tones as in the combustor, correspond to the rotational speeds and multiples thereof of the turbomachinery. A narrow band spectrum taken at 40% of design speed but at a much wider frequency range, 0 to 10,000 Hz, is shown in figure 9. There are strong tones in evidence which correspond to the blade passage frequencies of the impeller, turbine and fan. In addition, there are some oscillations between 7000 and 9000 Hz which remain yet to be explained.

Far field - Directivity patterns taken from existing data for low frequency core engine noise indicate a maximum in the vicinity of 120° from the engine inlet (Ref. 2). Far field acoustic spectra at this angle are presented in figure 10. In figure 10(a), one-third octave band sound pressure level spectra are given for five engine speeds. A constant band-width spectrum to 10,000 Hz at 40% of design speed as shwon in figure 10(b) indicates the presence

of many tones. These tones are the fundamentals and harmonics of the blade passage frequencies of the fan, the impeller and the turbine. At 87% of design speed, the far field sound pressure level spectrum shown in figure 10(c) contains a region of multiple pure tones, and three distinct tones. All of these tones are caused by the fan. The three distinct tones correspond to the fan blade passage frequency and its second and third harmonics. The multiple pure tones may be caused by a combination of phenomena such as inlet flow distortion and rotor stator interaction.

Acoustic Power - The variation of low frequency acoustic power as a function of jet exhaust velocity is shown in figure 11. The acoustic power level was computed from signals between 50 and 2000 Hz, the region where broadband core and jet noise propagate to the far field. The far field acoustic power was computed in the usual manner from the microphone data. The acoustic power at the core nozzle exit was computed, on the assumption of an acoustic plane wave, as the product of the acoustic intensity and the area of the duct at the probe location. The intensity, I, for a moving stream is expressed in reference 9 as:

$$I = \frac{\overline{p}^2}{\rho c} (1 + M) \qquad (2)$$

where

$\overline{p}^2$ local mean square pressure fluctuation

ρ local density

c local speed of sound

M local Mach number

The core nozzle exit acoustic power level shown in figure 11 was computed from the following equation which is a product of a transformation of eq. (2), and the core nozzle exit area

$$PWL = SPL + 47.58 + 10 \log_{10} \frac{A\sqrt{T}}{p} (1 + M) \qquad (3)$$

where

PWL sound power level, dB, ref. 10^{-13} watts

SPL sound pressure level measured by probe, dB, ref. 2×10^{-5} Pa

A area (square meters)

T temperature (K)

p pressure (pascals)

The effective jet exhaust velocity, V_E, given in figure 11 is arbitrarily defined for convenience as a simple measure of engine operating condition. It is a weighted velocity which accounts for the differences in mass flow and velocity of the fan and core at each engine condition, and is defined as:

$$V_E = \frac{BPR \cdot V_F + V_C}{BPR + 1} \tag{4}$$

where

V_F fan velocity

V_C core velocity

BPR engine by-pass ratio

It can be seen in figure 11 that in the low velocity region (up to approximately 175 m/sec) the power level calculated at the core engine exit is in close agreement with the power level calculated in the far field at 30.5 m. However, above 175 m/sec the power level in the far field becomes considerably greater (10 dB at 300 m/sec) than the level in the nozzle exit region. Also, above an effective jet exhaust velocity of 175 m/sec the far field acoustic power behaves approximately as velocity to the eighth power which is indicative of jet mixing noise. This suggests strongly that below a critical engine operating condition (65% of design speed in this case) where the jet noise is not significant, noise emanating from the engine core is a significant if not dominant contributor to the far field noise.

Coherence Measurements

In order to better understand the dynamic pressure characteristics within the engine core, two point coherence functions were made between internal and far field engine measurements, and between pairs of internal measurements.

The coherence function is essentially a normalized cross-spectrum and is defined for random signals as (Ref. 10)

$$\gamma^2_{ab}(f) = \frac{|G_{ab}(f)|^2}{G_{aa}(f)\, G_{bb}(f)} \tag{5}$$

where $|G_{ab}(f)|^2$ is the square of the ensemble averaged cross-spectral density between a and b; and $G_{aa}(f)$ and $G_{bb}(f)$ are the averaged autospectral densities at a and b, respectively. The coherence function must hava a value between zero and one, with high coherence at a particular frequency, f, meaning high correlation at that frequency.

Herein, the coherence function will be used primarily to describe the pairwise frequency characteristics of the fluctuating pressure within the JT15D engine. The magnitude of the coherence function will be referred to in relative terms and will be used mainly for comparison purposes. For the engine presented in this paper the coherence is virtually zero above 1000 Hz. Therefore, for the sake of uniformity, coherence measurements will be presented only between 0 and 1000 Hz, and analyzed with a resolution bandwidth of 2 Hz. All bias errors due to time delay between internal and far field measurements were corrected according to the methods presented in reference 3. Bias errors due to time delay between internal measurements are negligible.

Combustor - The measured coherence functions between pressure in the combustor and several downstream stations for an engine speed of 40% are shown in figure 12. As discussed in the previous section and shown in figures 5(b) and 8(b) there are tones in the engine whose frequencies correspond to turbomachinery rotational speeds. These tones retain their coherence between the various

measuring stations inside and outside of the engine, and appear as highly coherent "spikes" in the measured coherence functions. For clarity, they have been edited out of the figures. In figure 12(a) the measured coherence between the fluctuating pressure in the combustor and the turbine exit station is shown. There is a single distinct region of coherence between 0 and 250 Hz and negligible coherence above 250 Hz. The magnitude of the coherence function reaches a peak at approximately 140 Hz. In figure 12(b), the measured coherence between combustor and core nozzle exit is shown to have similar characteristics. In addition, figure 12(c) shows the measured coherence function between the fluctuating pressure in the combustor and the far field acoustic pressure at a microphone located 120° from the engine inlet. As can be seen from the figure, the coherence between the combustor pressure and the far field acoustic pressure is limited to the region below 250 Hz, the same as between pressures within the engine.

Using the coherence measurement as a guide, a filtered cross correlation function between the combustor pressure and the acoustic far field has been measured (Fig. 13). This filtered correlation exhibits the property of being symmetric about a negative peak and therefore cannot be associated with pure time delay. A correlation function with these same characteristics was obtained between combustor and far field on a YF 102 engine in an earlier experiment (Ref. 2). It has been shown in reference 2, that for the frequency range where the fluctuating combustor pressure is coherent with the far field acoustic pressure, the combustor is a source region for far field noise.

In summary, combustor related noise measured in the JT15D engine and in the far field is limited entirely to the frequency range below 250 Hz with a peak between 125 and 150 Hz.

Turbine exit - The measured coherence function between pressure in the turbine exit and two downstream locations for an engine speed of 40% of maximum is shown in figure 14. In figure 14(a), the coherence between the fluctuating pressure in the turbine exit station and the core nozzle exit station is shown. There are three regions of coherence between 0 and 1000 Hz: one between 0 and 250 Hz; a second between 250 and 500 Hz; and a third between 500 and 1000 Hz. In figure 14(b), which shows the measured coherence between the fluctuating pressure in the turbine exit and the acoustic pressure in the far field, the third region of coherence has diminished almost to zero while the two lower frequency regions of coherence are still very strongly in evidence. Because the region of coherence above 500 Hz is weak between the turbine exit and the core nozzle exit and almost zero between the turbine exit and the far field, it will not be discussed in this paper. The low frequency region of coherence, between 0 and 250 Hz, is most likely caused by the combustor related noise propagating through the engine to the far field (Fig. 12). The second region of coherence, between 250 and 500 Hz, must be originating at some point downstream of the combustor. The three stage turbine is downstream of the combustor and just upstream of the turbine exit station. It is the most likely source of noise in this coherence region.

Core nozzle exit - The measured coherence function between pressure in the core nozzle exit and the 120^{o} far field microphone is shown in figure 15 for two engine speeds. In figure 15(a), the coherence between the fluctuating pressure in the core nozzle exit and the far field location is shown for an engine speed of 40%. There is one continuous region of coherence between 0 and approximately 700 Hz. Within this coherence range there are included the previously discussed combustor noise (0 to 250 Hz) and turbine noise (250 to 500 Hz). In addition, in the region above 200 Hz, based on the magnitude of the coherence function, there are additional noise sources which most likely

occur upstream of the core nozzle exit. These additional sources may be caused by the struts in the turbine exit duct and scrubbing in the core nozzle. In figure 15(b), coherence between pressure in the core nozzle exit and far field is shown for an engine speed of 87%. At this high engine speed, the coherence is very low in value at all frequencies. This low level of coherence is due to contributions to the far field noise from sources other than those within the core nozzle. Specifically, these other contributions are the mixing noise from the core and fan exhausts which occur downstream of the core nozzle exit.

In summary, based on these coherence measurements, noise sources within the core nozzle make a significant contribution to the far field at low engine speed and a negligible contribution at high engine speed. These coherence data, at both speeds, are in agreement with the results of the acoustic power calculations presented in figure 11.

Comparisons with YF102 Engine

The results obtained from the JT15D measurements are compared now with those obtained previously from a YF102 engine (Refs. 1 to 3), both engines being in the same size class. The YF102 engine is used to power the NASA Quiet Shorthaul Research Aircraft (QSRA) and is the earlier version of the AVCO/Lycoming ALF 502 which powers general aviation aircraft such as the Canadair Challenger. Both engines have reverse flow annular combustors of very similar size, but have compressors, turbines and core nozzles which are different in design. The JT15D engine has a single stage compressor and a three stage turbine whereas the YF102 has an eight stage compressor and a four stage turbine.

A comparison of combustor acoustic power level as a function of heat release rate for the JT15D and the YF102 combustors is presented in figure 16. The ordinate, acoustic power level, has been normalized to account for the seven percent difference in cross sectional area between the two combustors. All of

the YF102 combustor data, including that obtained at its lowest engine operating point, are above the two megawatt heat release rate and the acoustic power behaves approximately as Q to the first power. The acoustic power levels are in excellent agreement with the present JT15D combustor data for comparable heat release rates.

Measured coherence functions between pressure in the combustor and the far field, at 120^{o}, for both engines at comparable speeds (approximately 40%) are shown in figure 17. In both cases, there is a single distinct region of coherence between 0 and 250 Hz and negligible coherence above 250 Hz. The magnitude of the coherence function reaches a peak between 125 and 150 Hz for both engines.

In figure 18 are shown measured coherence functions between dynamic pressure in the core nozzle exit and the far field at low speed for both engines. In the region below 200 Hz, there is very good agreement in the measured data between the two engines. However, above 200 Hz, based on the coherence measurements, the JT15D engine propagates a much greater signal to the far field than the YF102 engine. The agreement below 200 Hz can be accounted for by the strong similarities between the two combustors, and the disagreement above 200 Hz is probably due to the differences in design of the turbine,struts and core nozzle. For both engines, at high speed, the coherence level between core nozzle exit pressure and far field signal is very low at all frequencies. This low level of coherence is due to contributions to the far field noise from sources other than those within the core nozzle, specifically, jet mixing noise.

SUMMARY OF RESULTS

Core noise from a JT15D turbofan engine was investigated using simultaneous measurements of internal pressure and far field noise. Acoustic wave-

guide probes were located in the combustor, at the turbine exit and in the core nozzle.

From direct internal and external measurement, low frequency acoustic power determined at the core nozzle exit corresponds in level to the far field acoustic power at engine speeds below 65% of maximum. At engine speeds above 65% of maximum, the jet noise dominates in the far field, greatly exceeding that of the core. Pairwise coherence measurements between core nozzle exit and far field at low frequency corroborate that acoustic sources within the core nozzle make a significant contribution to the far field noise at low engine speed and a negligible contribution at high engine speed. At high frequencies, above 2000 Hz, core tones and their harmonics from the impeller and turbine are very evident in the far field at low engine speed. At high engine speed, the far field noise is dominated by sources originating at the fan, multiple pure tones and blade passage frequencies, and the core tones are hardly noticeable.

From internal and far field coherence and correlation measurements, it has been determined that the combustor is the dominant source of the low frequency core noise and is limited to the region below 250 Hz with a peak between 125 and 150 Hz. A second region of coherence originating downstream of the combustor, between 250 and 500 Hz, is most likely associated with the turbine.

Within the combustor it has been shown that the acoustic power behaves as approximately heat release rate, Q, to the second power at low values of Q and as heat release rate to the first power at high values of Q.

The results obtained from the JT15D measurements have been compared with those previously obtained from a YF102 engine. The combustor related measurements, both internal and those propagating to the far field, are very similar for the YF102 and JT15D engines. The good agreement is most probably due to the similarity in combustor design between the two engines. On the other hand,

based on coherence measurements, there is poor agreement between the two engines at low operating speed in the frequency range where combustor noise does not dominate (above 200 Hz). This disagreement is most likely due to the different characteristics of the engine components downstream of the combustor. At high engine speed, jet mixing noise dominates the far field signal for both engines.

REFERENCES

1. M. Reshotko, A. Karchmer, P. F. Penko, and J. G. McArdle, "Core Noise Measureme , on a YF102 Turbofan Engine," AIAA Paper 77-21 (Jan. 1977); also J. Aircr. 14, (7) 611-612 (Synoptic) (1977).
2. A. Karchmer and M. Reshotko, "Core Noise Source Diagnostics on a Turbofan Engine Using Correlation and Coherence Techniques," NASA TM X-73535 (Nov. 1976).
3. A. M. Karchmer, M. Reshotko, and F. J. Montegani, "Measurement of Far Field Combustion Noise from a Turbofan Engine Using Coherence Functions," AIAA Paper 77-1277 (Oct. 1977).
4. P. N. Shivashankara, "Gas Turbine Core Noise Source Isolation by Internal-to-Far-Field Correlations," J. Aircr. 15, (9) 597-600 (1978).
5. W. L. Jones, J. G. McArdle, and L. Homyak, "Evaluation of Two Inflow Control Devices for Flight Simulation of Fan Noise Using a JT15D Engine," AIAA Paper 79-0654 (Mar. 1979).
6. J. G. McArdle, W. L. Jones, L. J. Heidelberg, and L. Homyak, "Comparison of Several Inflow Control Devices for Flight Simulation of Fan Tone Noise Using a JT15D-1 Engine," AIAA Paper 80-1025 (June 1980).
7. J. C. Plucinsky, "'Quiet' Aspects of the Pratt & Whitney Aircraft JT15D Turbofan," SAE Paper 730289 (April 1973).
8. U. H. von Glahn, "Correlation of Combustor Acoustic Power Levels Inferred from Internal Fluctuating Pressure Measurements," NASA TM 78986 (1978).

9. D. C. Pridmore-Brown, "Sound Propagation in a Fluid Flowing through an Attenuating Duct," J. Fluid Mech., 4, (4) 393-406 (1958).

10. J. S. Bendat and A. G. Piersol, Engineering Applications of Correlation and Spectral Analysis (Wiley, New York, 1980).

TABLE I. - TEST CONDITIONS FOR THE JT15D CORE NOISE MEASUREMENT PROGRAM

Nominal engine speed, % of maximum	Fan speed, rpm	Core speed, rpm	Core mass flow, kg/sec	Compressor exit		Combustor		Core nozzle	
				Pressure, kPa	Temperature, K	Pressure, kPa	Temperature, K	Pressure, kPa	Temperature, K
33	5 195	15 745	2.33	177	395	171	826	101	675
37	5 785	17 230	2.50	196	404	190	849	101	682
40	6 305	18 435	2.73	214	413	208	869	102	687
44	6 975	19 855	3.03	241	422	234	886	102	694
55	8 665	22 820	3.76	314	449	305	942	105	717
62	9 855	24 485	4.34	372	467	361	980	106	736
68	10 792	25 675	4.82	420	482	407	1 021	109	754
73	11 590	26 625	5.21	465	493	451	1 059	111	772
87	13 850	28 895	6.62	612	529	593	1 162	120	816
97	15 360	30 650	7.79	729	556	707	1 257	128	878

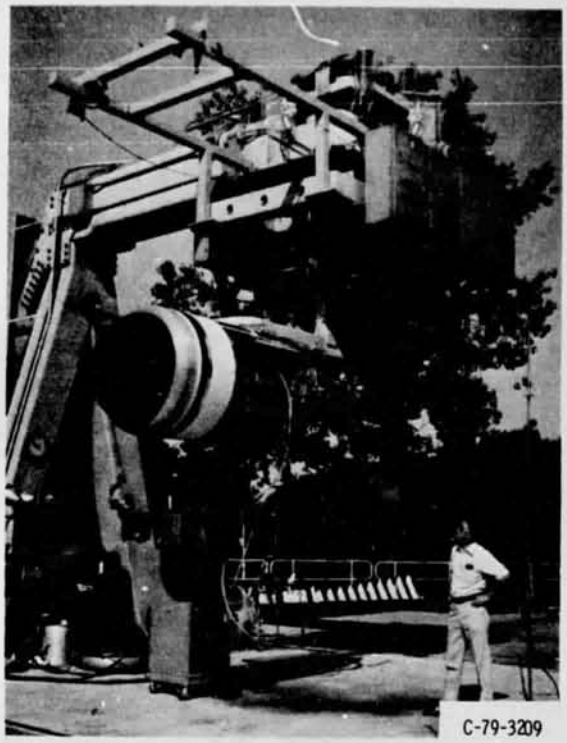

Figure 1. - JT15D turbofan engine on test stand.

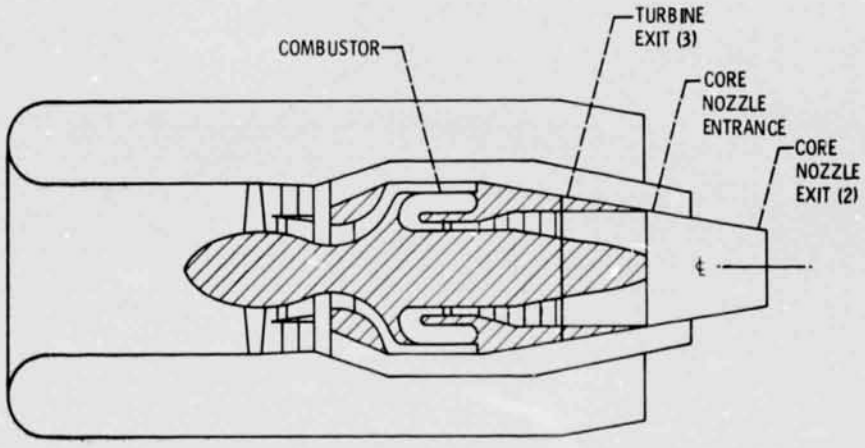

Figure 2. - Core acoustic waveguide probe locations.

Figure 3. - JT15D turbofan engine with acoustic waveguide probes installed.

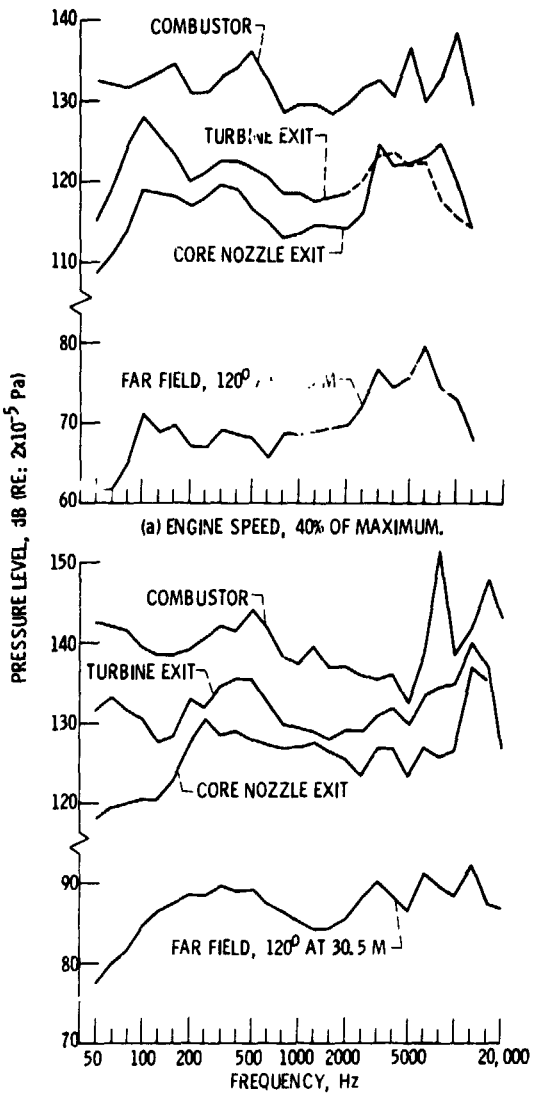

(a) ENGINE SPEED, 40% OF MAXIMUM.

(b) ENGINE SPEED, 87% OF MAXIMUM.

Figure 4. - JT15D internal and far field pressure level spectra.

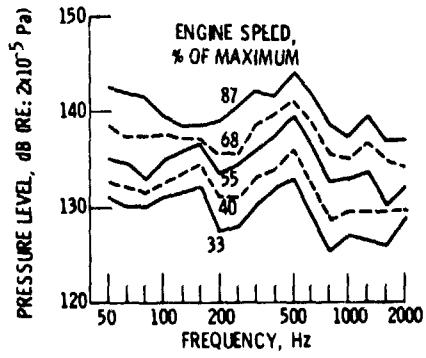

(a) ONE-THIRD OCTAVE BAND SPECTRA.

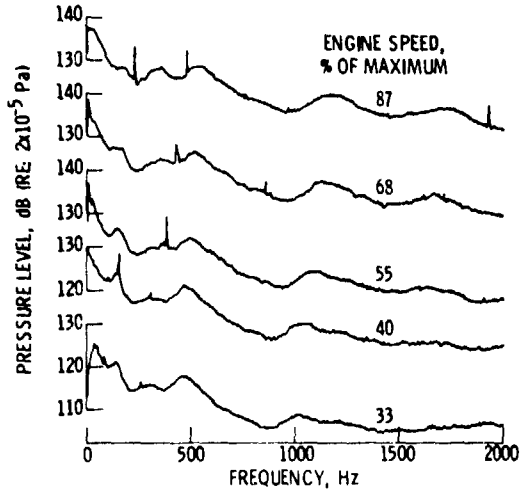

(b) NARROW BAND SPECTRA. FILTER BANDWIDTH, 2.5 Hz.

Figure 5. - Combustor pressure spectra.

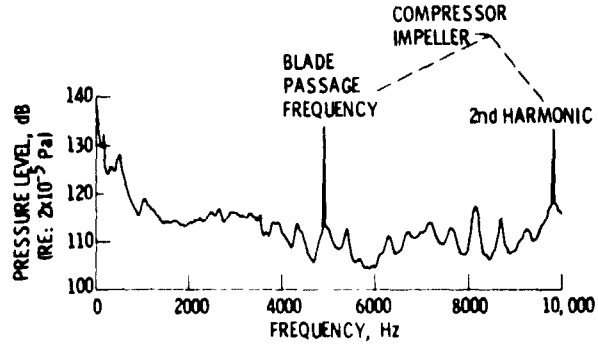

Figure 6. - Combustor pressure spectrum. Engine speed, 40% of maximum; filter bandwidth, 12.5 Hz.

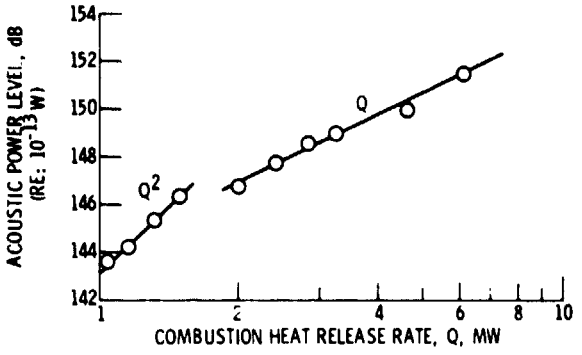

Figure 7. - Variation of combustor acoustic power level with heat release rate.

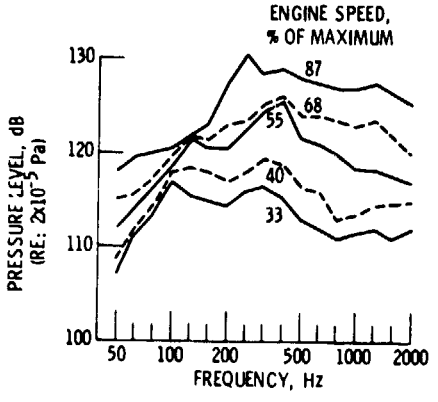

(a) ONE-THIRD OCTAVE BAND SPECTRA.

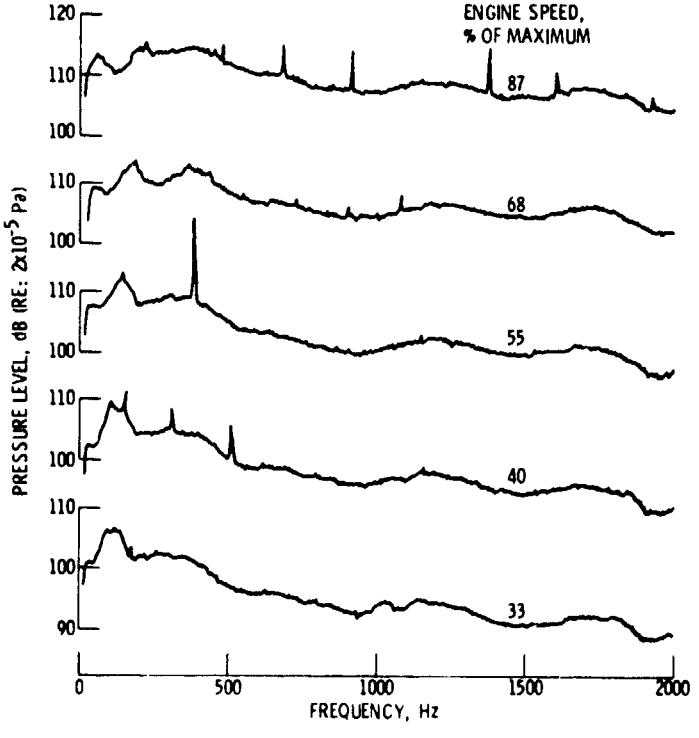

(b) NARROW BAND SPECTRA. FILTER BANDWIDTH, 2.5 Hz.

Figure 8. - Core nozzle exit pressure spectra.

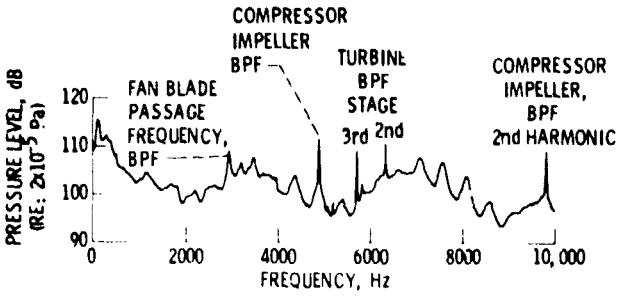

Figure 9. - Core nozzle exit pressure spectrum. Engine speed, 40% of maximum; filter bandwidth, 12.5 Hz.

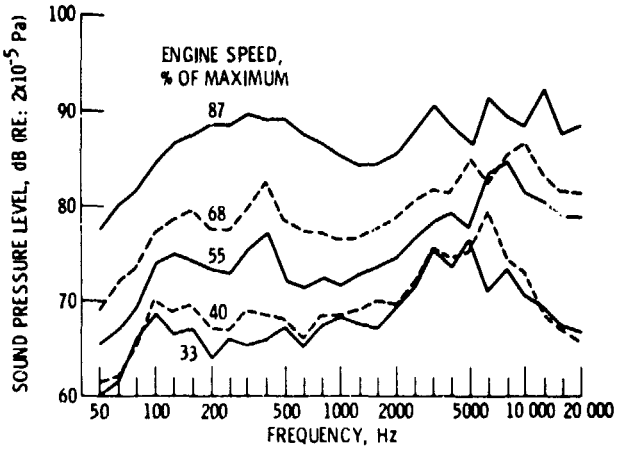

(a) ONE-THIRD OCTAVE BAND SPECTRA.

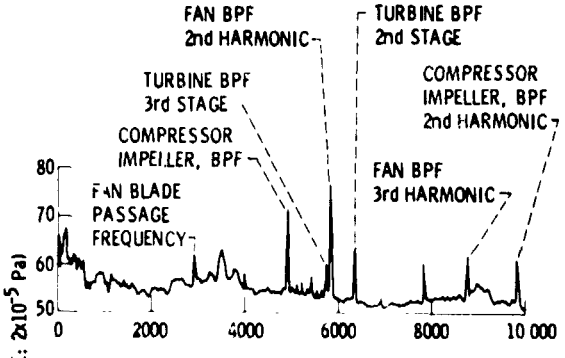

(b) NARROW BAND SPECTRUM. ENGINE SPEED, 40% OF MAXIMUM; FILTER BANDWIDTH, 12.5 Hz.

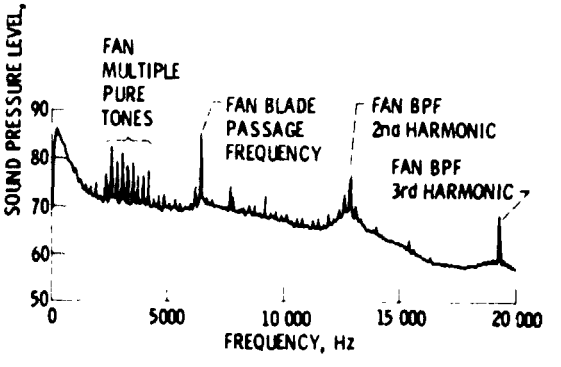

NARROW BAND SPECTRUM. ENGINE SPEED, 87% OF MAXIMUM; FILTER BANDWIDTH, 25 Hz.

Figure 10. - Far field acoustic spectra. Distance, 30.5 M; angle from engine inlet axis, 120°.

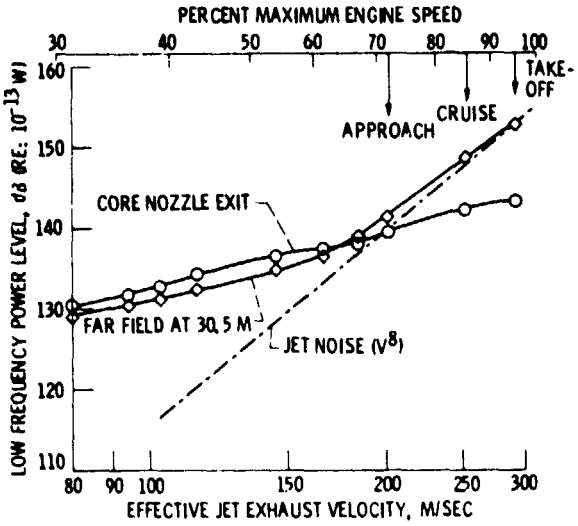

Figure 11. - JT15D low frequency acoustic power.

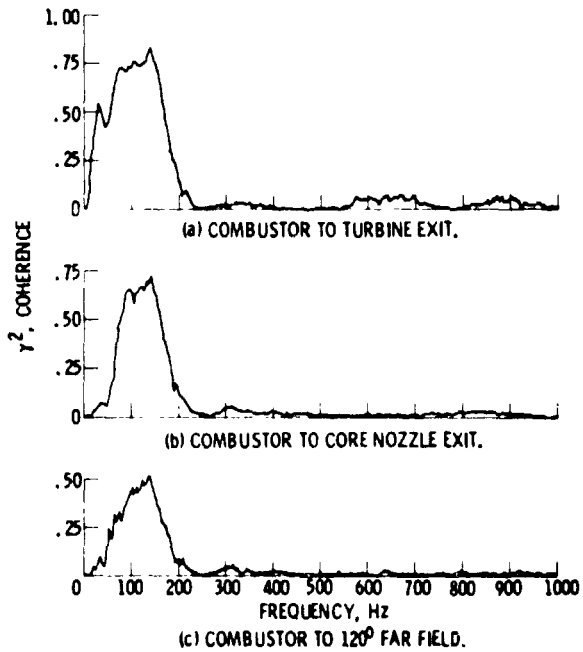

Figure 12. - Coherence between fluctuating combustor pressure and several downstream locations. Bandwidth, 2 Hz.

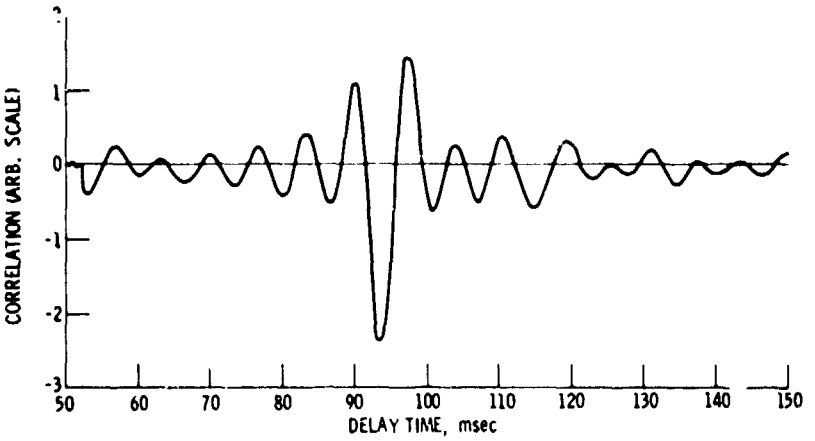

Figure 13. - Cross correlation between combustor and far field signals. Engine speed, 40% of maximum; data low pass filtered at 240 Hz; angle from engine inlet axis, 120°.

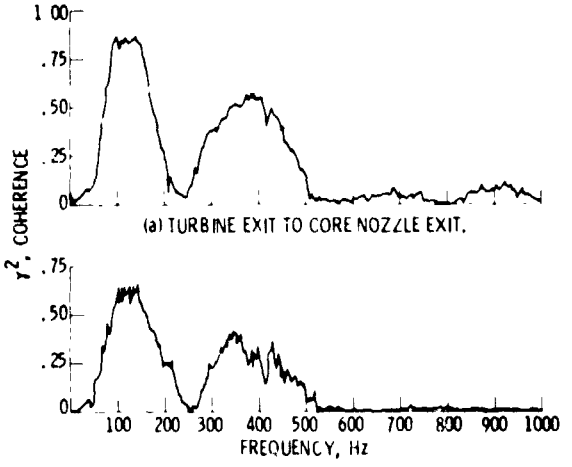

(b) TURBINE EXIT TO 120° FAR FIELD.

Figure 14. - Coherence between fluctuating pressure at the turbine exit and two downstream locations. Bandwidth, 2 Hz.

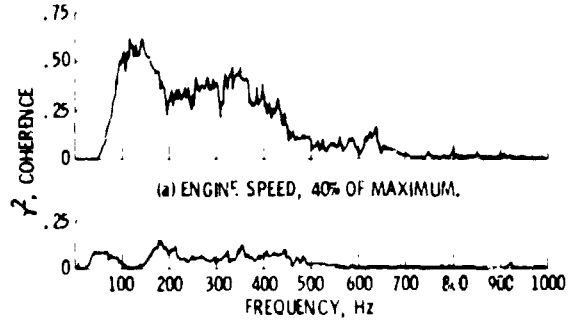

(b) ENGINE SPEED, 87% OF MAXIMUM.

Figure 15. - Coherence between fluctuating pressure at the core nozzle exit and the acoustic far field. Bandwidth, 2 Hz; angle from engine inlet axis, 120°.

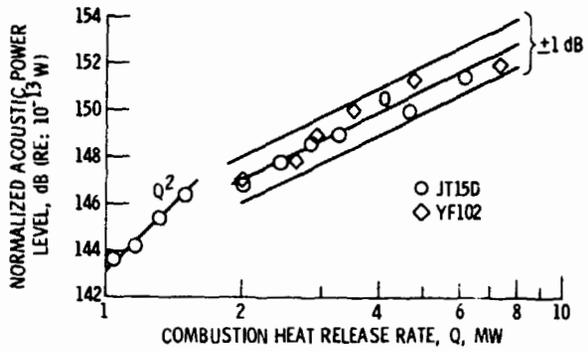

Figure 16. - Comparison of combustor acoustic power level between the JT15D and YF102 reverse flow annular combustors.

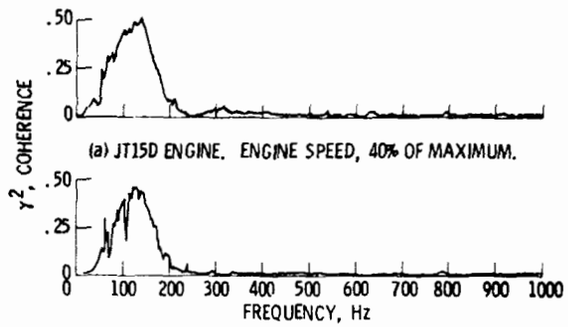

(b) YF102 ENGINE. ENGINE SPEED, 43% OF MAXIMUM.

Figure 17. - Comparison of combustor to far field coherence between the JT15D and YF102 engines. Bandwidth, 2 Hz; angle from engine inlet axis, 120°.

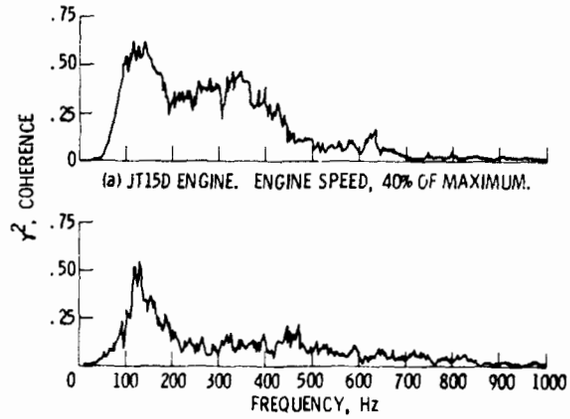

(b) YF102 ENGINE. ENGINE SPEED, 43% OF MAXIMUM.

Figure 18. - Comparison of core nozzle exit to far field coherence between the JT15D and YF102 engines. Bandwidth, 2 Hz; angle from engine inlet axis, 120°.